Scripta Materialia 157 (2018) 106–109

Contents lists available at ScienceDirect

Scripta Materialia

journal homepage: www.elsevier.com/locate/scriptamat

Regular article

Experimental and numerical analysis of residual stress in carbon-stabilized expanded austenite

Yawei Peng [a,b,c], Zhe Liu [a,b], Yong Jiang [a,b], Bo Wang [c], Jianming Gong [a,b,*], Marcel A.J. Somers [c]

[a] School of Mechanical and Power Engineering, Nanjing Tech University, No.30 Puzhu South Road, Nanjing 211816, China
[b] Jiangsu Key Lab of Design and Manufacture of Extreme Pressure Equipment, No.30 Puzhu South Road, Nanjing 211816, China
[c] Department of Mechanical Engineering, Technical University of Denmark, Produktionstorvet b. 425, 2800 Kgs. Lyngby, Denmark

ARTICLE INFO

Article history:
Received 30 June 2018
Received in revised form 6 August 2018
Accepted 6 August 2018
Available online xxxx

Keywords:
Expanded austenite
Surface treatment
Residual stress
X-ray diffraction
Numerical analysis

ABSTRACT

Expanded austenite obtained by gaseous carburizing of stainless steel was investigated with X-ray diffraction to determine composition-depth and residual stress-depth distributions. Avoiding ghost stress effects in the analysis of X-ray diffraction data, the obtained composition- and stress-depth profiles are in excellent quantitative agreement with those obtained with other techniques. The residual stress-depth profile was attempted calculated from the composition-depth profile assuming elastic-plastic accommodation of the lattice expansion. In the model, composition-dependence of Young's modulus, yield stress and work hardening exponent were considered. Excellent quantitative agreement was achieved between the experimental and numerical residual stress-depth profiles.

Low-temperature thermochemical surface engineering of austenitic stainless steels through carburizing (<800 K), nitriding or nitrocarburizing (<715 K) has been demonstrated to significantly improve the tribological/wear and fatigue performance, as well as improving the resistance against localized corrosion [1–7]. The origin of these improvements is a case of expanded austenite, which essentially is a supersaturated solid solution of interstitial carbon or nitrogen atoms in austenite [8,9]. Although the present work concentrates on carbon-stabilized expanded austenite, the case developing on nitriding and nitrocarburizing is analogous; the main difference is that nitrogen can reach a substantially higher supersaturated solid solubility in austenite, because of the stronger interaction of Cr with N than with C atoms [10]. After low-temperature surface carburizing and nitriding, compressive residual stresses of several GPa's are present in the developed case. Due to the shallow case depth (few tens of microns) and the change from several GPa's compression to virtually zero stress over the case depth, it is challenging to accurately determine the quantitative values of the residual stresses. The X-ray diffraction (XRD) $\sin^2\psi$ method is a widely applied technique to determine residual stresses by measuring the lattice strains and was also applied to carbon-stabilized expanded austenite [7,8,11–13]. Generally, for thermochemical surface engineering characterized by 1-dimensional (in depth) diffusion into a flat sample, the stress state is plane stress ($\sigma_{13} = \sigma_{23} = \sigma_{33} = 0$) and rotationally symmetric ($\sigma_{11} = \sigma_{22} = \sigma_{//}$). Lattice strains ε_ψ^{hkl} experienced by the set of lattice planes {*hkl*} in a direction defined by tilt angle ψ is given by [14]:

$$\varepsilon_\psi^{hkl} = \frac{d_\psi^{hkl} - d_{\varepsilon=0}^{hkl}}{d_{\varepsilon=0}^{hkl}} = \frac{1}{2} S_2^{hkl} \sigma_{//} \sin^2\psi + 2S_1^{hkl}\sigma_{//} \quad (1)$$

where d_ψ^{hkl} and $d_{\varepsilon=0}^{hkl}$ are the strained and strain-free (reference) lattice spacings, respectively. S_1^{hkl} and $\frac{1}{2}S_2^{hkl}$ are the X-ray elastic constants.

Consequently, the lattice spacing along the depth-direction z can be expressed as:

$$d_\psi^{hkl}(z) = d_{\varepsilon=0}^{hkl}(z)\left[1 + \sigma_{//}(z)\left(\frac{1}{2}S_2^{hkl}\sin^2\psi + 2S_1^{hkl}\right)\right] \quad (2)$$

Taking K as the slope of d_ψ^{hkl} vs. $\sin^2\psi$ plots, the stress-depth profile can be straightforwardly calculated as:

$$\sigma_{//}(z) = \frac{K}{\frac{1}{2}S_2^{hkl} d_{\varepsilon=0}^{hkl}(z)} \quad (3)$$

where $d_{\varepsilon=0}^{hkl}(z)$ follows from inserting $\sin^2\psi_{\varepsilon=0} = -2S_1^{hkl}/\frac{1}{2}S_2^{hkl}$ in Eq. (2).

It should be noted that the lattice spacings determined by XRD analysis represent an intensity-weighted average value over the diffracting volume below the surface and depends on the geometry of the

* Corresponding author at: School of Mechanical and Power Engineering, Nanjing Tech University, No.30 Puzhu South Road, Nanjing 211816, China.
E-mail address: gongjm@njtech.edu.cn (J. Gong).

https://doi.org/10.1016/j.scriptamat.2018.08.006
1359-6462/

diffraction set up (Bragg angle 2θ, tilt angle ψ, and, optionally, a grazing incidence angle) and the combination of sample composition and applied wavelength. Straightforward application of the $\sin^2\psi$ method without taking the stress and, in particular, composition gradients within the sampled volume into consideration, leads to artifacts in the determined stress values, so-called ghost stresses [15]. To avoid ghost stresses, Somers et al. [15,16] proposed a procedure where the actual residual stress profile is evaluated after reconstruction of the lattice spacing profiles for each of the ψ directions investigated and was applied to carburized stainless steel in Ref. [9]. Rong et al. [17] determined residual stresses in the low-temperature carburized case based on a nano-indentation technique proposed by Suresh et al. [18]. This method is more complicated compared to XRD method, but it does not lead to ghost stresses. Alternatively, numerical analysis can be applied to predict residual stresses in expanded austenite. A first attempt to numerically predict residual stresses in expanded austenite from elastic-plastic accommodation of the composition-induced lattice expansion was recently put forward by Jespersen et al. [19].

In this work, AISI 316L (in at.%: 0.12 C, 18.14 Cr, 9.69 Ni, 1.17 Mn, 0.95 Si, 1.16 Mo, balance Fe) was treated by low-temperature gaseous carburizing at 743 K for 30 h. Details of the low-temperature gaseous carburizing process were described elsewhere [20]. Residual stresses were determined by the PROTO-iXRD residual stress analyzer using the $\sin^2\psi$ method with Mn K_α X-radiation ($\lambda = 0.210314$ nm). Lattice strains were probed for the 311 austenite reflection, because this *hkl* is least sensitive for plastic deformation in lattice strain determination [21]. The applied X-ray elastic constants were $S_1^{311} = -1.76 \times 10^{-6}$ MPa^{-1}, $\frac{1}{2}S_2^{311} = 7.07 \times 10^{-6}$ MPa^{-1} [9] and assumed independent of the composition. Five ω tilt angles were applied corresponding with $\sin^2\psi$ values ranging from 0 to 0.4. For depth profiling, thin layers were successively removed by careful grinding and polishing unto a final step of 3.5 μm diamond paste. In order to avoid ghost stresses, the method firstly proposed in Ref. [15], was applied, involving:

(1) The experimental assessment of $\langle d_\psi^{hkl}(\Delta z)\rangle$ vs. Δz profiles, where Δz is the total thickness removed.
(2) Reconstruction of $d_\psi^{hkl}(z)$ profiles for all investigated values of ψ from $\langle d_\psi^{hkl}(\Delta z)\rangle$ vs. Δz profiles:

$$d_\psi^{hkl}(z)\Big|_{x=y} = \left\langle d_\psi^{hkl}(\Delta z)\right\rangle - \left.\frac{\partial\left\langle d_\psi^{hkl}(\Delta z)\right\rangle}{\partial z}\right|_y \cdot \left[\frac{1-\exp(-A_\psi\cdot(Z_l-\Delta z))}{A_\psi}\right] \quad (4)$$

where Z_l is the (original) layer thickness for the case where layer and substrate can be distinguished with XRD. If layer and substrate cannot be distinguished by XRD, Z_l should be replaced by half the sample thickness (for expanded austenite, Z_l is the sample thickness, i.e., effectively infinitely large). A_ψ is the absorption factor for the X-ray diffraction geometry under consideration. For an Ω-type goniometer as applied here, the absorption factor is:

$$^{\Omega}A_\psi = \mu\left[\frac{1}{\sin(\theta+\psi)} + \frac{1}{\sin(\theta-\psi)}\right] \quad (5)$$

where μ is the linear absorption coefficient of the X-radiation used in the sample investigated, which was taken as 0.075 μm^{-1}.

(3) Reconstruction of d_ψ^{hkl} vs. $\sin^2\psi$ plots at the various depths z and determination of the strain-free lattice parameter $d_{\varepsilon=0}^{hkl}(z)$ for the strain-free direction and calculation of the stress from Eq. (3).

The composition-depth and residual stress-depth profiles thus determined are given in Fig. 1. For comparison also the profiles obtained without appropriate reconstruction are given. Evidently, the reconstructed carbon contents and compressive residual stress values are much larger than the "uncorrected" values; in the steepest part of the profiles an underestimation of the composition and stress by up to 1.72% C and 1.0 GPa, respectively, results if no appropriate data evaluation is made. For comparison the composition profile obtained by electron probe microanalysis (EPMA) [22] and the residual stress-depth profile obtained by Rong et al. [17] with nano-indentation for a sample carburized under identical conditions, are given in Fig. 1 for comparison. Excellent agreement is obtained between the independent techniques. After reconstruction, a maximum compressive residual stress of −2.65 GPa is obtained at the surface, for a maximum carbon content of 11.7 at.% C; similar values were found in Ref. [9] for gaseously carburized AISI 316, albeit under different conditions. Clearly, the determined residual stress values are beyond the uniaxial yield stress of AISI 316L (292 ± 5 MPa, as measured in uniaxial tension). It should be noted that the dissolution of carbon atoms in the austenite lattice contributes appreciably to strengthening of the lattice [23]. In previous work, it was found that the Young's modulus, E, yield stress, σ_y, and work hardening exponent, n, assessed (at room temperature) by nano-indentation all depend on the carbon content in expanded austenite [24]. The data showing the composition dependence is summarized in Fig. 2. Although, the yield strength is enhanced spectacularly, eventually the competition between strengthening by carbon dissolution and composition-induced stress leads to plastic deformation (see also discussion in Ref. [9], where this was already pointed out). This is consistent with the observation of extensive slip bands at the surface of austenitic stainless steel after low-temperature surface carburizing [7,25].

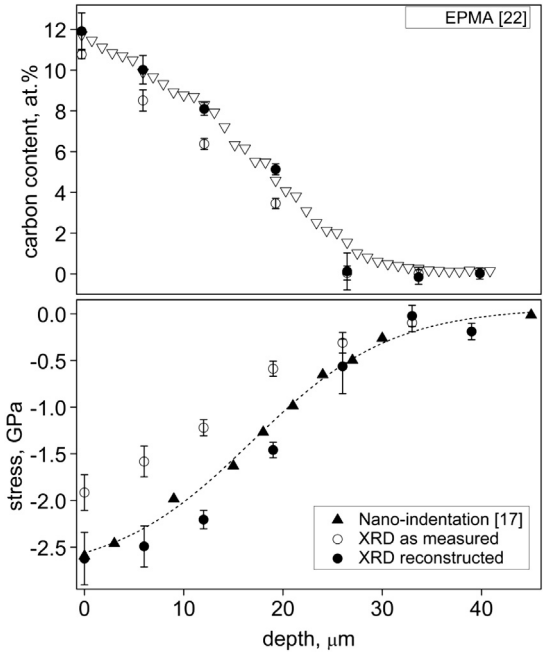

Fig. 1. Experimental composition-depth and residual stress-depth profiles of AISI 316L carburized at 743 K for 30 h, determined with XRD analysis with and without ghost stress correction, EPMA and nano-indentation (EPMA data from Ref. [22] and nano-indentation data from Ref. [17]). The dashed line is a sigmoidal fit through the nano-indentation data.

During low-temperature carburizing no phase transformation occurs [8]. Although carbon is expected to have some effect on the thermal expansion coefficient of austenite, this effect is negligible as long as no magnetic transition occurs on cooling [26]. Therefore, the total strain ε_{ij}^{tot} in the carburized sample is the sum of the mechanical strain ε_{ij}^{mech} and the composition-induced strain ε_{ij}^{c}, which is given by:

$$\varepsilon_{ij}^{tot} = \varepsilon_{ij}^{el} + \varepsilon_{ij}^{pl} + \varepsilon_{ij}^{c} \quad (6)$$